Team Members: Joshua Close, Bryan Perschbacher, Sean Reilly, Hunter Stevens, Jonathan Thong, Etienne Viaud-Murat, Stephen Wormald

Faculty Advisor: George Qin, Ph.D.

School of Engineering & Computer Science, Cedarville University, Cedarville, OH 45314

Design and Fabrication of a Remote-Controlled Hydrofoil Prototype

ABSTRACT

A remote-controlled hydrofoil prototype has been designed, fabricated and tested by the 2018-2019 Cedarville University hydrofoil senior design team. This project was the first step toward a human-powered hydrofoil boat. The prototype adopted a catamaran configuration of two hulls connected to a middle frame. A canard layout of three hydrofoils were used to generate lift. Two Shutt struts were employed to adjust the angle of attack of the two front hydrofoils for pitch and roll control. An above-water fan powered by an electric motor was utilized to drive the prototype. The motor was remote-controlled. The prototype design is shown in Figure 1.

Figure 1: Cedarville Hydrofoil Prototype

In the design phase, extensive analytical and numerical analyses were carried out to evaluate the performance of the prototype designs. Parameters including weight, buoyancy, lift, drag, thrust, power, and takeoff speed were calculated for each iteration of design.

Once the design was finalized, proper materials were selected to fabricate the prototype components. The manufacturing process was made efficient with the aid of advanced CAD tools like SolidWorks and modern manufacturing techniques such as CNC machining and 3D printing.

Numerous tests were then carried out and the prototype subsystems worked as designed. Stable flight was realized with the prototype.

INTRODUCTION

The MIT human-powered hydrofoil boat Decavitator set the world-record of speed in 1991 (Wall, 1995). It is desirable to create a similar boat that is comparable with or even outperform Decavitator at Cedarville University. As the first step toward this end, the 2018-2019 Cedarville hydrofoil senior design team decided to design and build a half-scale hydrofoil boat prototype. The goal of the project was to realize steady flight with the prototype.

Before more details of the project are discussed, it should be helpful to overview the relationship of the various forces involved in the operation of the hydrofoil prototype.

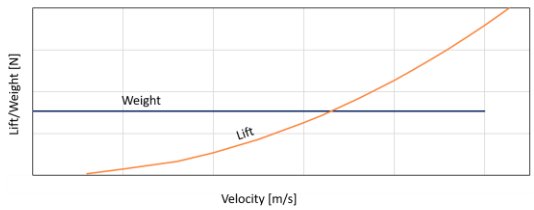

Figure 2: Lift vs. Velocity

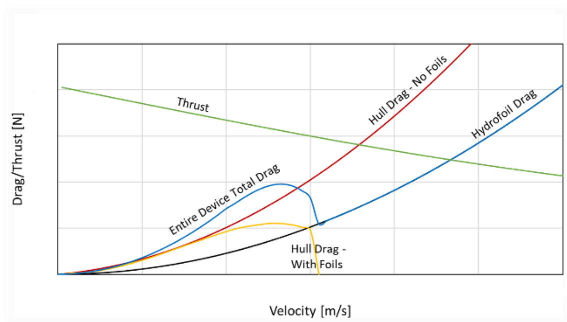

Figure 3: Drag and Thrust vs. Velocity

As Figure 2 shows, the lift force generated by the hydrofoils increases with increasing velocity following a quadratic equation, which is a well-known fact (Munson, 2016). The drag force acting on the underwater portion of the prototype would have a similar dependency on velocity had the volume of this portion stayed constant.

The overall weight of the prototype is balanced by the lift force and the buoyancy due to the underwater portion of the prototype. As velocity increases the lift force grows and the prototype rises up, hence the buoyancy drops and the vertical force balance is still maintained. The reduction in the underwater portion of the prototype results in a tendency of decreasing of the drag force which gradually overtakes the trend of drag growth with increasing velocity. As a result a "hump" appears on the drag force curve as shown in Figure 3. Obviously the thrust force produced by the fan must be higher than the drag hump so that the prototype can be lifted out of the water and fly. Another condition for the takeoff of the prototype is of course that the lift force must exceed the overall weight at the takeoff speed. Due to the mutual dependency of the forces, the design of different components of the prototype, say the hulls and hydrofoils was necessarily interactive and iterative.

To design a dynamic system like the current one, not only should one guarantee the balance of forces so that the system may work, one also has to assure any small deviation from the normal state of the system can be corrected. Such considerations are termed as stability analysis. For our hydrofoil prototype, the moments produced by pitching and rolling has to be controlled so that a steady flight is possible.

Such pitch and roll control were realized partially by the catamaran configuration of two hulls before takeoff. Whenever small pitching or rolling occurs, the change of the buoyancy distribution on the two hulls helps restore the original state. When the prototype is lifted out of the water, special ways has to be implemented to achieve pitch and roll stability. In our system two Shutt struts connected to the two front hydrofoils were applied for this purpose. More details are given in the corresponding sections.

SPECIFICATIONS

We used the parameters of the MIT human-powered hydrofoil boat Decavitator (Wall, 1995) as the guidance to determine the specifications of our half-scale prototype.

The overall length of Decavitator is 20 ft, therefore we used a value of 96 in, which was close to one half of the length of Decavitator as the overall length of our prototype.

The overall weight of Decavitator is 48 lb. Since the weight of a geometry is roughly proportional to the cube of its size, we might expect a half-size Decavitator to weigh around 48/8 = 6 lb. A half-size human rider from the wonderland should drive such a half-size boat. In order to estimate the weight of such an imaginary rider, who was assumed to be an athlete, we collected the weight and height data of about 200 Olympic game players, as summarized in Figure 4 and Figure 5.

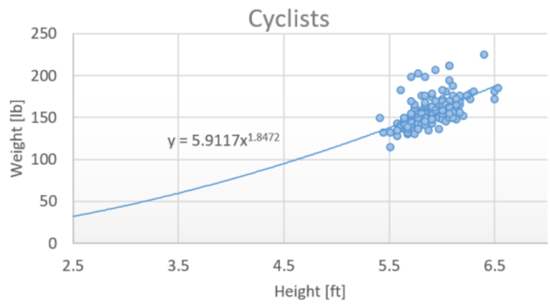

Figure 4: Weight and Height Data of Olympic Cyclists

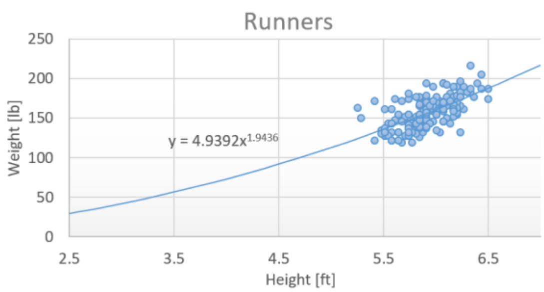

Figure 5: Weight and Height Data of Olympic Runners

We then concluded from the curve fitting of these data that the weight of this imaginary half-size (about 3 ft tall) athlete would be about 42 lb. Therefore the overall weight of our hydrofoil prototype should be close to 42 + 6 = 48 lb so that it could simulate the half-size boat and the wonderland rider on board. To be prudent, we required that our prototype should weigh 50 lb.

The peak cruise speed of Decavitator is about 9.5 m/s, we used 60% of it, that is 5.7 m/s as the target takeoff speed of our full-size hydrofoil boat. To specify the takeoff speed of the half-scale prototype, we used Froude number similarity between the full-size boat and the prototype, which requires the Froude numbers to be the same for each of them at similar operational states. For most cases involving fluid flow, Reynolds number similarity is the best choice (Munson, 2016). For surface vessels like catamaran hulls, Froude number similarity is a better choice because the Froude number captures the effects of wave drag (Munson, 2016). The Froude number Fr is defined based on the hull depth l, the gravitational acceleration g, and the boat speed V (Munson, 2016):

$$Fr = \frac{V}{\sqrt{gl}} \qquad (1)$$

The Froude number similarity thus implies $V \propto \sqrt{l}$. Therefore the takeoff speed of the half-scale prototype should be about $\frac{5.7\ m/s}{\sqrt{2}} = 4\ m/s$.

Another specification needed to be determined was the fan power at the drag hump. For the full-size human-powered hydrofoil device, the power source is the human power. A professional athlete can output a peak power between 1200 W and 1500 W (Ikonen, 2011). The fan power is equal to

$$P = \frac{T \cdot V}{\eta} \approx \frac{D \cdot V}{\eta} = \frac{C_d \cdot \frac{1}{2}\rho V^2 A \cdot V}{\eta} \qquad (2)$$

where T is the thrust force; D, C_d and A are the drag force, the drag coefficient, and the wetted area of the prototype, respectively; ρ is the water density and η is the fan efficiency. Since $A \propto l^2$, $V \propto \sqrt{l}$, we may conclude that $P \propto l^{\frac{7}{2}}$ if we ignore the variation of η with the fan size. Hence the power budget for the half-scale prototype should be about $\frac{0.5(1200+1500)\ W}{2^{3.5}} = 120\ W$. It was also clear that the maximum drag force the hull experiences close to takeoff should not exceed $\frac{120\ W}{4\ \frac{m}{s}} = 30\ N$.

HULL DESIGN

To design the hull shape, we had to find the drag force on the hull. Once we knew the drag force, we could modify the hull shape until the required drag force specification was met.

In order to calculate the drag force on the hull, we had to first know the water surface location (water level) at different boat speeds. This information was obtained by applying the vertical force balance, that is lift L plus buoyancy B

equals weight W. As lift equals weight at takeoff, one may easily find that

$$\frac{L}{W} = \frac{C_l \cdot \frac{1}{2}\rho V^2 A}{C_l \cdot \frac{1}{2}\rho V_{takeoff}^2 A} = \left(\frac{V}{V_{takeoff}}\right)^2 \qquad (3)$$

So the buoyance force is

$$B = W\left[1 - \left(\frac{V}{V_{takeoff}}\right)^2\right] \qquad (4)$$

which equals the weight of water displaced by the underwater portion of the hull:

$$W\left[1 - \left(\frac{V}{V_{takeoff}}\right)^2\right] = \rho \cancel{V}_{underwater} \qquad (5)$$

It was then straightforward to find the volume of the underwater portion of the hull and in turn the water level at any given velocity.

We calculated the drag force with three methods. The first method was using the computational fluid dynamics (CFD) software FLUENT to simulate the flow over the prototype. The second method was using the CFD package of SolidWorks called Flow Simulation to do the flow field calculation. FLUENT is generally believed to be more accurate than SolidWorks Flow Simulation as FLUENT simulates both the water flow and the air flow above the water yet SolidWorks Flow Simulation can only handle a single phase flow, say the water flow. However a FLUENT simulation takes much longer time to run than a SolidWorks simulation. Therefore we used SolidWorks to quickly iterate hull shapes and using FLUENT only for the final hull design to give accurate force predictions. The last method to predict the drag force was an analytical method which is described with the following example.

Figure 6 shows one of the hull designs. In order to model the drag on the hull analytically, several assumptions were made. Firstly we treated the sides of the hull as flat plates of the same length as the hull. This assumption is justified because the length of the hull is much large than its width. The bottom of the boat was modeled as a flat plate with 75% of the length of the hull to take into account the curvature of the bow.

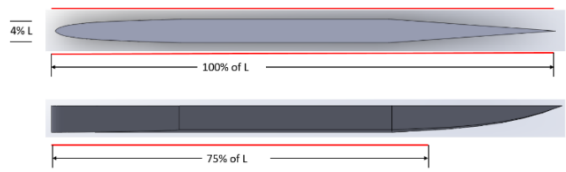

Figure 6: A Hull Design (Top: Top View, Bottom: Side View)

Using this model, we found the friction drag on the hull with the friction drag coefficient formulas for flow over flat plate surface which can be found in any standard fluid mechanics textbook like (Munson, 2016).

We also found the form drag on the hull. To do this, we assumed that the form drag coefficient of the hull would be the average of the drag coefficients of the airfoil and the ellipse at the same Reynolds number because the hull shape was more streamlined than the ellipse but less than the airfoil. The form drag coefficient of different geometries again can be found from (Munson, 2016).

These two components of drag were then added together to produce our analytical drag prediction for the hull.

The analytical predictions were compared to the numerical data from SolidWorks simulation results in Table 1. The percent difference between the predictions of these two methods was less than 5% over the velocity range between 1 m/s and 7 m/s.

Table 1: Comparison between SolidWorks Simulation and Analytical Prediction of Drag

Speed (m/s)	**Drag (N) Predicted by SolidWorks Simulation**	**Drag (N) Predicted by Analytical Model**	**Percent Difference**
1	2.8	2.9	4.6

2.5	15.7	15.9	1.1
3	22.0	22.4	1.8
4	36.9	38.4	4.1
5	59.0	58.5	0.9
6	80.3	82.5	2.7
7	107.5	110.4	2.7

With the help of the SolidWorks Flow Simulation and the analytical model, we were able to iterate numerous hull shapes as shown in Figure 7.

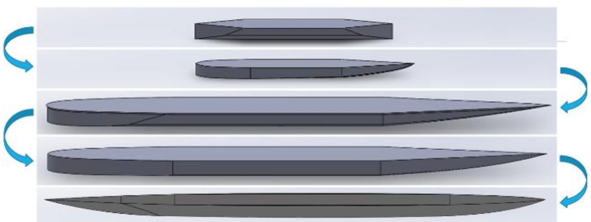

Figure 7: Iterations of Hull Shape Designs

FLUENT was then used to investigate the final hull design. For this purpose, a mesh system was created for the CFD simulation. A relatively coarse mesh was used except close to the prototype, where a very fine mesh was applied. In this way the simulation could be made both time efficient and accurate. The mesh system is shown in Figure 8 and Figure 9.

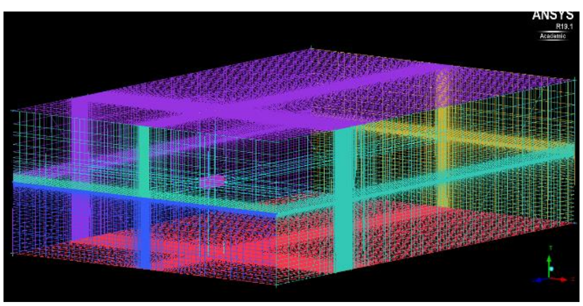

Figure 8: The Coarse Mesh

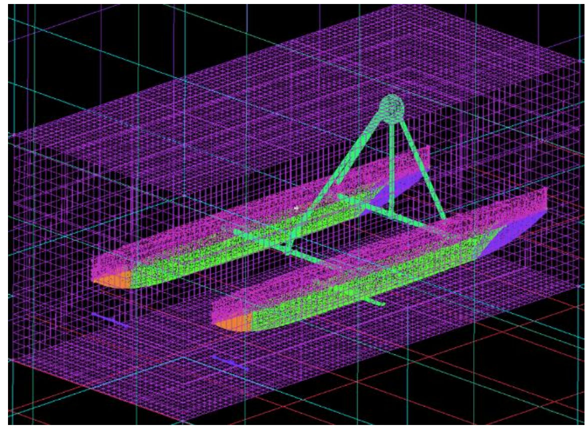

Figure 9: The Fine Mesh

The results are shown in Figure 10. As one may observe, the FLUENT results agree relatively well with the theoretical predictions of the drag and lift forces. And the final design of the hull shape satisfied all the specifications we set: the takeoff speed was 3.9 m/s < 4 m/s and the drag hump was at 22 N < 30 N.

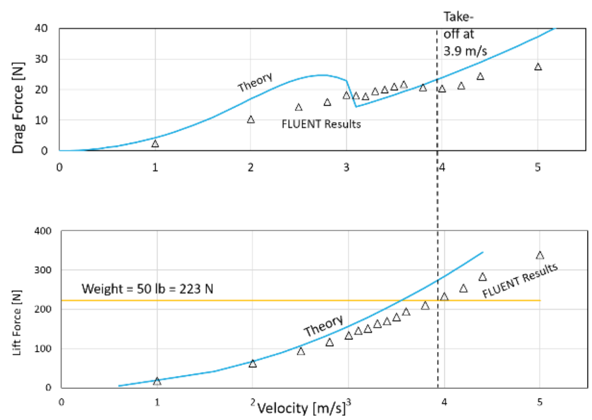

Figure 10: FLUENT Simulation Results

HYDROFOIL DESIGN

We decided to use a canard hydrofoil configuration consisting of three hydrofoils to support the boat. One main hydrofoil sat slightly behind the center of gravity of the entire boat and two smaller hydrofoils sat at the very front of each hull. The main rear hydrofoil was designed to do most of the lifting work, ranging anywhere from eighty to ninety percent of the load. The two front hydrofoils bore the remaining load while acting as pitch and roll control devices when attached to the surface finding mechanisms.

We used the hydrofoil theory equations to evaluate the lift and drag of various hydrofoil profiles. These equations like Equations (2) and (3) could be found from (Vellinga, 2009). Using these equations, we were able to give approximate values of lift and drag based on hydrofoil characteristics such as chord length, span, taper ratio, aspect ratio, and angle of attack as well as fluid characteristics such as density, viscosity and flow velocity.

The NACA 4412 profile was chosen for all our hydrofoils because it gave a balance between high lift to drag ratio and manufacturability. Taper was adopted to reduce the induced drag due to wing tip vortices.

The final design of the hydrofoils is summarized in Table 2.

Table 2: Hydrofoil Dimensions and Performance Data

Parameter	**Front hydrofoil**	**Rear hydrofoil**
Airfoil Section	NACA 4412	NACA 4412
Average Chord Length	2.85 cm	7.0 cm
Span	26.0 cm	66.5 cm
Aspect Ratio	9.1	9.5
Taper Ratio	0.63	0.71
Lift Coefficient	0.462	0.636
L/D Ratio during Cruise	13.3	13.0
Angle of Attack during Cruise	6.7°	6°

The final hydrofoil design would be able to support the estimated 50lb prototype in flight, which was verified by the SolidWorks CFD simulation. The simulated flow field around the rear hydrofoil is shown in Figure 11.

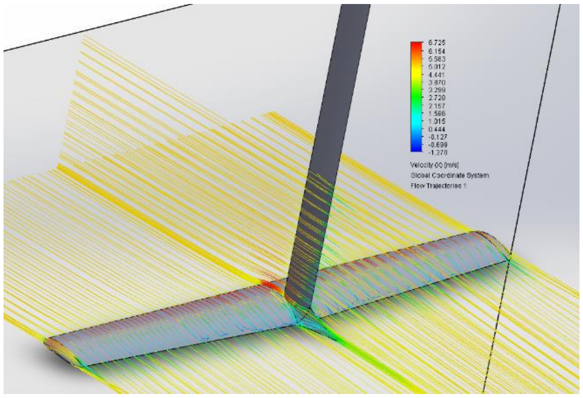

Figure 11: SolidWorks Simulated Flow Field

The drag and lift forces of the rear hydrofoil at the takeoff speed predicted by SolidWorks are shown in Figure 12, which agree well with the hydrofoil theory and FLUENT simulation results.

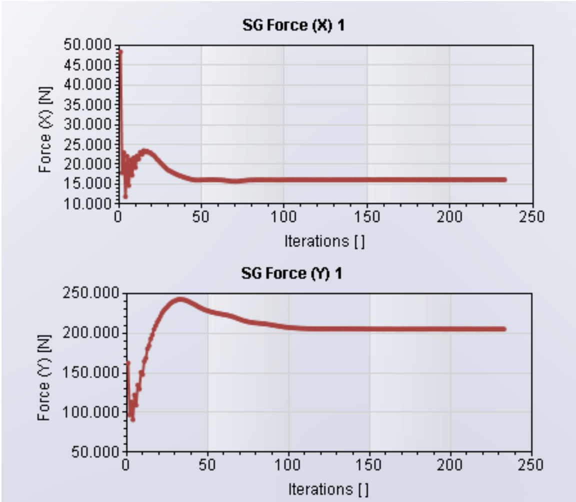

Figure 12: Drag (Top) and Lift (Bottom) of the Rear Hydrofoil at Takeoff Velocity

For the hydrofoil strut design we decided to choose a symmetrical hydrofoil cross-section shape in order to reduce the strut drag. To calculate the stress experienced by the struts, we modeled the strut cross-sections as rectangular beams as shown in Figure 13 and used the Euler criteria for buckling to estimate the approximate strut thickness needed given the expected weight and length of the struts (Vellinga, 2009). Based on the analysis we decided on the NACA 0020 section profile which minimized the strut drag and maximized the ability of the strut to withstand stresses.

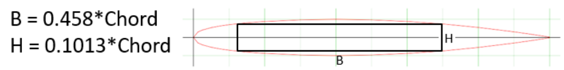

Figure 13: Strut Model

SURFACE FINDING MECHANISM DESIGN

As mentioned in the introduction section, stability of our boat prototype was a big concern. The largest stability problems came from controlling the moments created by pitching and rolling of the boat.

To control pitch, usually devices with some form of a height adjuster that manipulates the amount of lift of the hydrofoils were used. The most common solution to height adjustment involves using a fixed angle joint between the hydrofoil strut and an arm connected to a water surface following body. At the chosen cruising height, the variable-angle hydrofoils are at their designed angle of attack. If the boat goes above or below the desired height, the surface finder mechanically adjusts the angle of attack of the hydrofoils and their resultant lift to bring the boat back to the target height.

In order to determine the arm length and the angle between the arm and strut, we used a two-dimensional geometric analysis including the desired flying height, the strut length, and the range of angle of attacks needed to get anywhere from no lift to maximum lift. We designed a system as shown in Figure 14 to control the pitch and height of the prototype by controlling the angle of attack of the front hydrofoils. The system is essentially a Shutt strut (Vellinga, 2009).

Figure 14: Surface Finding Mechanism Design

At the lowest height of the hull when the boat is motionless, the surface finder gives the front hydrofoil an angle of attack of 13.5°. This is less than the stall angle of the hydrofoil, which is approximately 16°. When flying at the cruise height, the surface finder gives the front hydrofoil an angle of attack of approximately 7°. This value provides enough lift to keep the hulls out of the water.

This mechanism is also used for roll control when the prototype is lifted out of the water. As one side of the boat rises higher than the other side, the surface finder on the rising side will reduce the angle of attack and the lift of the hydrofoil on that side which lowers that side. Similarly the surface finding mechanism will raise the lower side. These actions help restore the original state of the boat. However, in order to make sure that this mechanism alone is enough to control rolling, the distance between the two front hydrofoils must be properly calculated with a roll stability analysis.

Figure 15 sketches the front view of the boat prototype and the roll control mechanism.

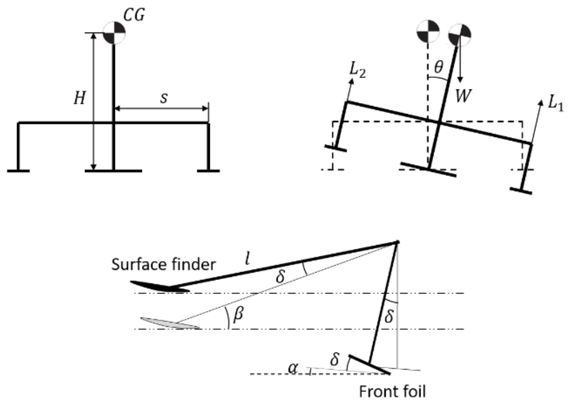

Figure 15: Sketch of Roll Control

As the boat rolls for a small angle θ from the desired upright state, the surface finders immediately cause the lift forces of the two front hydrofoils to change. The lower side front hydrofoil then has a greater lift L_1 than the higher side front hydrofoil, which has a smaller lift L_2. If we focus on the lower side front hydrofoil, we may find that this lift adjustment is realized by the surface finder increasing the angle of attack of the hydrofoil from its original value α to $\alpha + \delta$ as shown in Figure 15. δ is the rotation angle of the surface finder arm in this process. At the same time the angle of attack of the rising side hydrofoil changes from α to $\alpha - \delta$. To be roll stable, the restoring moment has to exceed the rolling moment:

$$(L_1 - L_2)s \geq WH \cdot \sin\theta \approx WH \cdot \theta \qquad (6)$$

in which s is the half distance between the two front hydrofoils and H is the distance between the center of gravity and the rear hydrofoil.

From geometric consideration, one may find that the displacement of each surface finder in this process is

$$l \cdot \cos\beta \cdot \delta \approx s \cdot \sin\theta \approx s \cdot \theta \qquad (7)$$

where l is the surface finder arm length and β is the angle between the surface finder arm and the water surface.

Therefore

$$\delta \approx \frac{s}{l \cdot \cos\beta} \cdot \theta \qquad (8)$$

Since

$$\begin{cases} L_1 = C_{l1} \cdot \frac{1}{2}\rho V^2 A \approx \pi(\alpha + \delta) \cdot \rho V^2 A \\ L_2 = C_{l2} \cdot \frac{1}{2}\rho V^2 A \approx \pi(\alpha - \delta) \cdot \rho V^2 A \end{cases} \qquad (9)$$

as the lift coefficient of a thin hydrofoil is $C_l \approx 2\pi\alpha$ (Katz & Plotkin, 2001), the roll stability condition becomes

$$\begin{aligned}(L_1 - L_2)s &\approx 2\pi\delta\rho V^2 As \\ &\approx 2\pi \frac{s}{l \cdot \cos\beta} \cdot \theta \cdot \rho V^2 As \geq WH \cdot \theta\end{aligned} \qquad (10)$$

which infers a condition for the half-distance between the two front hydrofoils s:

$$s \geq \sqrt{\frac{WHl\cos\beta}{2\pi\rho V^2 A}} \qquad (11)$$

One may easily find that the parameters like β and V at takeoff give the most conservative criterion for s. For example, if $W = 50\ lb = 223\ N$, $H = 0.7\ m$, $l = 0.7\ m$, $V = 4\ m/s$, $\beta = 10°$ and $A = 0.007\ m^2$, the roll stability is only possible as $s \geq 0.39\ m$. That is the distance between the two front hydrofoils must be greater than 0.78 m to ensure roll stability.

FAN DESIGN

When designing the propulsion system for our boat, we first had to choose which propulsion method we would use. Our research showed that most vessels equipped with hydrofoils had used underwater propellers to drive their designs (Vellinga, 2009). Yet MIT Decavitator used an above-water fan to set the world-record for speed. For this reason, we decided to take a closer look at the three different options: a propeller, a dual fan and a single fan. The propeller had the advantage of being easily bought or manufactured on campus while being lightweight. We didn't pursue this option as we deemed having to attach both the main hydrofoil and the propeller system to the back strut would be too complicated for our manufacturing skills. A dual, counter rotating fan can provide rotating moment balance to the boat when in flight but once again, such a solution was too complex to manufacture on campus. Finally, we decided to take the simplest solution of a single fan.

Once the decision was made, we started looking at the fan dimension we would go for.

According to the actuator disk theory of fan (Johnson, 2013), the power of a fan is

$$P = \frac{1}{2} T \cdot V \left[\sqrt{\frac{T}{\frac{1}{2}\rho V^2 A_{disk}} + 1} + 1 \right] \qquad (12)$$

And its efficiency therefore is

$$\eta = \frac{2}{\sqrt{\frac{T}{\frac{1}{2}\rho V^2 A_{disk}} + 1} + 1} \qquad (13)$$

where T is the thrust force; V is the boat speed; ρ is the air density and A_{disk} is the area of the fan “disk” as what one sees as the fan rotates.

From this equation it is obvious that the larger the fan is, the more efficient it will be. Yet considerations such as overall weight, complexity of manufacturing, and negative effects of a high center of gravity on stability prevent us from pursuing a too large fan. Knowing the MIT Decavitator used a 3 m diameter fan, we decided to design a fan with a diameter of 1.25 m for our hydrofoil prototype.

According to the CFD results (see Figure 10) we knew we had to overcome about 22N of drag at takeoff. For this reason we decided to design a 1.25 m diameter fan that would output 30N of thrust at the boat speed of 4 m/s. With these specifications, one may find from Equation (12) the efficiency of such a fan would be close to 70%. Although very helpful to our design this result is only a good estimate as the actuator disk theory does not consider the effects of fan blade cross-section profile and flow rotation downstream the fan. For this reason we used OpenProp to design our fan as this software takes into consideration all the aforementioned effects.

We used the simple NACA 0010 profile as fan blade cross-section shape due to its easiness of manufacturing. The fan design OpenProp created is shown in Figure 16.

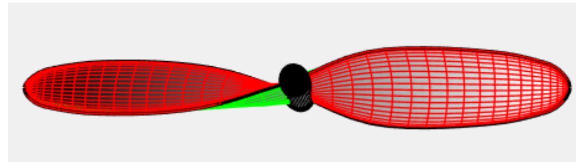

Figure 16: Fan Design

The fan efficiency curve is shown in Figure 17. The peak efficiency is 76% at the rotation speed 600 RPM, which was set as the target fan rotation speed.

The only problem of this design was that the power consumption of the fan was about $\frac{30\ N\cdot 4\frac{m}{s}}{76\%} = 158\ W$, which was higher than the power budget of 120 W due to the relatively low fan efficiency and the large margin in thrust force we required the fan to produce. This should not be a problem in the future as a fan is designed for the full-size boat as the fan efficiency increases with the fan size.

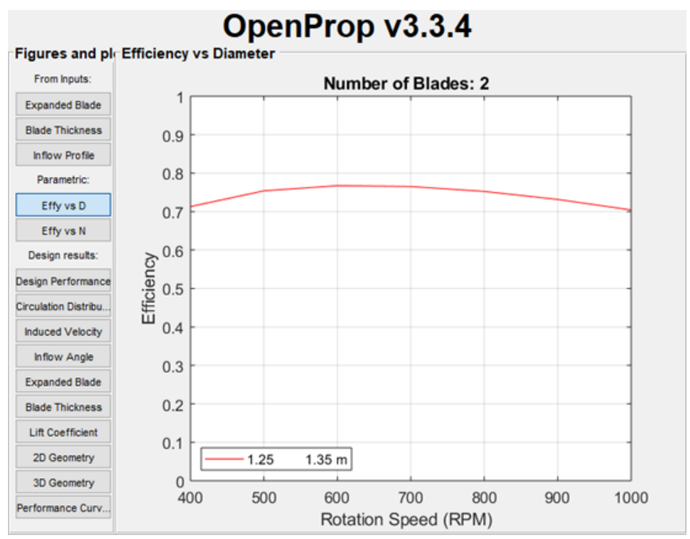

Figure 17: Fan Efficiency vs. Rotation Speed

A U8 Lite KV190 motor was used to drive the fan. The motor speed was remotely controlled by a FLYSKY remote control system. This motor produces 30 N of thrust at about 2000 RPM. We therefore needed a pulley system that would decrease our motor speed from 2000 RPM to 600 RPM for the fan.

To design such a system, the main variables were belt length, motor pulley diameter, fan pulley diameter, and distance between the pulleys. A TK Solver program was created to implement the geometric relationship between these variables. Our design sought to minimize the weight of the system by decreasing the component sizes. As the motor pulley could have a minimum diameter of about 2 in due to the fixture holes, a belt length of 29 in was selected as this minimized the distance between the pulleys while still allowing for a pulley ratio of 2000:600. The fan mount was designed as in Figure 18.

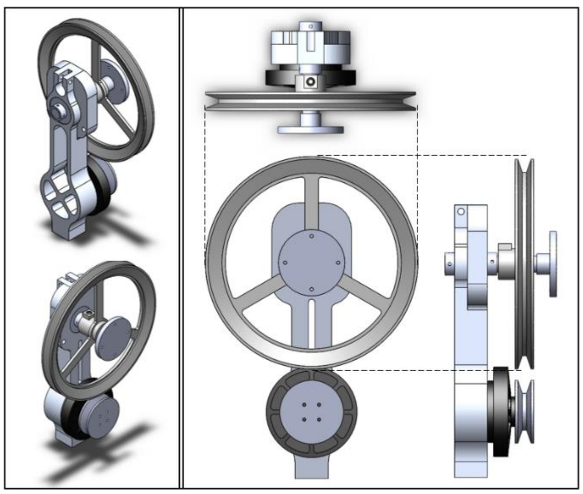

Figure 18: Fan Mount Design

Stress analysis was performed on the fan mount design as it was subject to significant stresses.

When setting up this simulation, a thrust of 30 N was applied to the front of the fan mount and the expected weight of the fan was applied in the downward direction. The stress distribution is seen in Figure 19. The simulation result revealed a safety factor greater than 5 for this design.

FRAME DESIGN

A frame was needed to hold the hulls together, to support the propulsion system (fan, motor, battery, remote control signal receiver etc.), to attach the rear hydrofoil, and to adjust the centers of lift and gravity if needed. This led to the design shown in Figure 20. The cross members fixed the hulls together, and the two members parallel to the hulls held the rear hydrofoil and electronics pod and allowed them to slide back and forth.

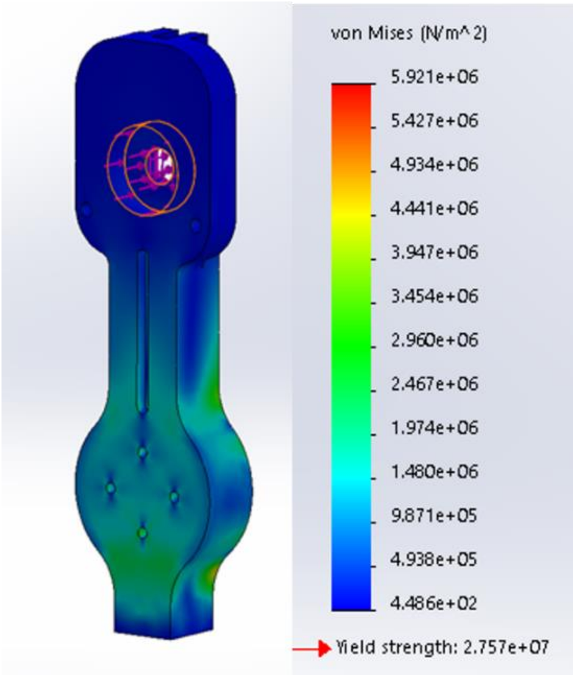

Figure 19: Stress Analysis of Fan Mount

A TK Solver program was composed to record the magnitude and point of impact of all the forces involved in all subsystems of the prototype. This program was then able to predict the location of the centers of lift and gravity. The attachment position of the frame on the hull was then determined accordingly to guarantee correct lift distribution among the hydrofoils.

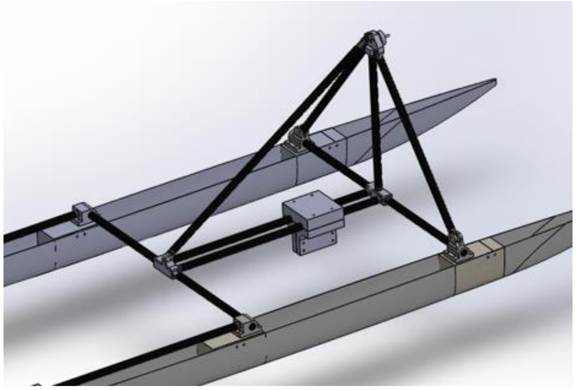

Figure 20: Frame Design

A connector that held the rear hydrofoil strut to the frame was also designed, see Figure 20. For simplicity of manufacturing, we decided to 3D print this part with ABS plastic.

When the boat is flying, the rear hydrofoil creates most of the lift. Therefore, the rear strut and connector hold most of the weight of the boat. A stress analysis was performed on this connector to ensure that it could withstand the stress. The load we gave on the rear strut in the analysis was 90% of the weight of the boat. A friction force 1.2 times the maximum expected value was applied to the connector's face. The results of this analysis are shown in Figure 21.

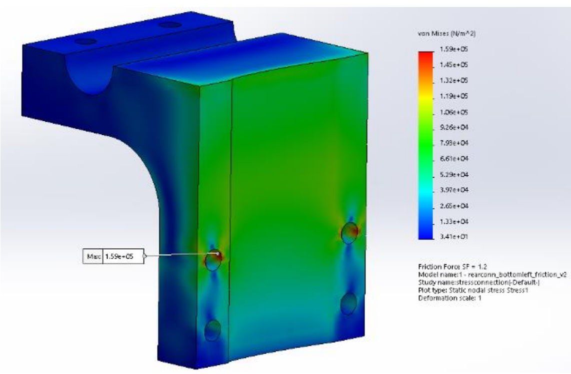

Figure 21: Stress Analysis of Rear Strut Connector

The maximum stress in the connector is only about 0.7 MPa, which is much less than the tensile strength of the ABS plastic which is about 20 MPa.

HULL FABRICATION

We began to manufacture the hull based on the design we had completed. We investigated several materials including fiberglass, balsa wood, and foam for our hull fabrication. The main manufacturing objectives were to minimize the weight and cost of the hulls and maximize the strength and surface finish quality. Each material has pros and cons.

Balsa wood is very light and is moderately expensive in standard sizes. However, for our eight-foot boat hulls, the wood would have to be custom made by laminating many smaller pieces of wood together. This would both make the wood much more expensive and increase the chances that the hull would fail by adding more joints. Foam is extremely light and inexpensive. However, it does not have the same strength as wood or fiberglass. It is much more likely to crack and break, unless it is reinforced with a coating of another material. Fiberglass was the material we chose for manufacturing. It is more expensive than foam, but comparable to balsa wood. It is slightly heavier than either of the other options, but it is much stronger than foam and has less laminations compared to balsa wood. This made fiberglass the best choice for our hulls.

Once we selected fiberglass, we had to choose a manufacturing method. We chose to create a female mold for our hull directly with the CNC router. We made two mold halves and clamped them together to create one mold. To cut the mold we laminated MDF boards into a feedstock larger than our hull size and used the router to cut the shape of the mold into the feedstock. Once the material had been cut, we sanded and smoothed the surface with an epoxy fairing putty. The fiberglass was then laid up into the mold and polyester resin was transferred to it by hand. Before the resin completely set, we rolled the fiberglass to eliminate air bubbles and surface imperfections.

The hulls are extremely long compared to the cross-sectional area, and this made them susceptible to deformation, especially in the transverse and torsional directions. To reduce such deflections and create a stronger hull, we added to it a 0.25 in thick foam core and an inner layer of fiberglass. A diagram of the completed cross section is shown in Figure 22.

The outer and inner layers of fiberglass were connected at the top of the hull above the foam core. A sheet of 0.25 in thick plywood was glued down to the top of the hull. This plywood sealed the hull, making it waterproof, and provided a surface for us to attach the hull to the frame. At the stern of the hull, a small hole was made, and a flexible tube and cork assembly was inserted into the hole in order to drain the hulls in case they did leak water.

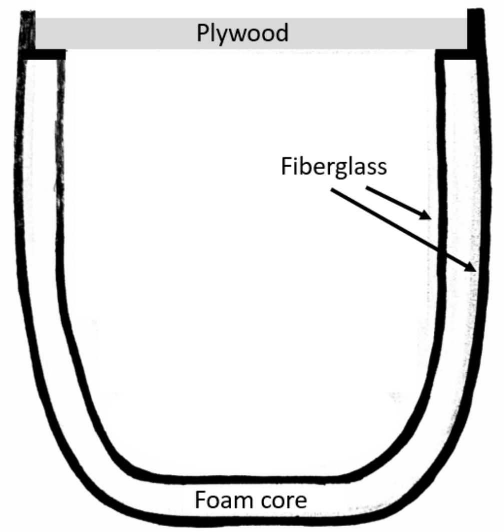

Figure 22: Diagram of Hull Cross Section

The completed hulls are shown in Figure 23.

HYDROFOIL FABRICATION

We researched aluminum, wood, and carbon fiber for hydrofoil fabrication. After considering factors such as cost, manufacturability, and strength to weight ratio we decided to produce the struts and hydrofoils out of aluminum using the CNC router at Cedarville as it was relatively easy and cost efficient. Making the hydrofoils and struts out of aluminum also gave us the ability to weld them together which avoided the need to design a more complicated attachment required for wood or carbon fiber hydrofoils and struts.

To manufacture the hydrofoils and struts we used aluminum stock at least 2 in longer and 1 in thicker than the strut or hydrofoil being manufactured. We would run a flat end mill with

Figure 23: Hulls

adaptive clearing to remove most of the material. And then a ball mill was used to give a nice finish to the strut. In order to machine the hydrofoils and struts properly we run the CNC on the top side of the stock and then flip it over and rerun the CNC on its bottom side.

The completed hydrofoils and struts are shown in Figure 24.

Figure 24: Hydrofoils and Struts

SURFACE FINDER FABRICATION

We used carbon fiber tubes to build surface finder arms as they are extremely strong yet very light.

Figure 25: Shutt Strut Joint

We had to design a joint that could connect the arm and strut rigidly to each other while allowing the entire assembly to pivot freely about a point on the hull to let the surface finder direct the movement of the hydrofoils. To keep the design simple, we designed the joint to be cut out of a metal sheet and bent it into a bracket-type joint, as shown in Figure 25. This design allowed us to use threaded fasteners to clamp the strut and arm tightly to their position. This design also allowed for a change in angle of the arm if needed.

The surface finder itself was made of fiberglass. The outer surface was created in the same way as the hulls: a female mold was created from MDF stock and was cut using the CNC router. The fiberglass was laid up by hand in two layers. The contour of the finder was then filled with foam to eliminate the possibility of water entering the finder (see Figure 14).

FAN FABRICATION

To build the entire propulsion system on campus, we decided to create the fan out of wood using the CNC router at Cedarville University. We decided to use Birch plywood because it is easily accessible and a previous senior design team (2015-2016 EPL fan team) had good results when creating their fan blades out of the same wood.

Using the SolidWorks guide curves output option of OpenProp, we quickly generated our blades in SolidWorks. We then glued 5 layers of 0.75 in plywood together into a feedstock. Afterwards the CNC was used to cut the feedstock into the fan blade shape. The procedure was very alike the one described in the hydrofoil fabrication section. The completed fan blade is shown in Figure 26.

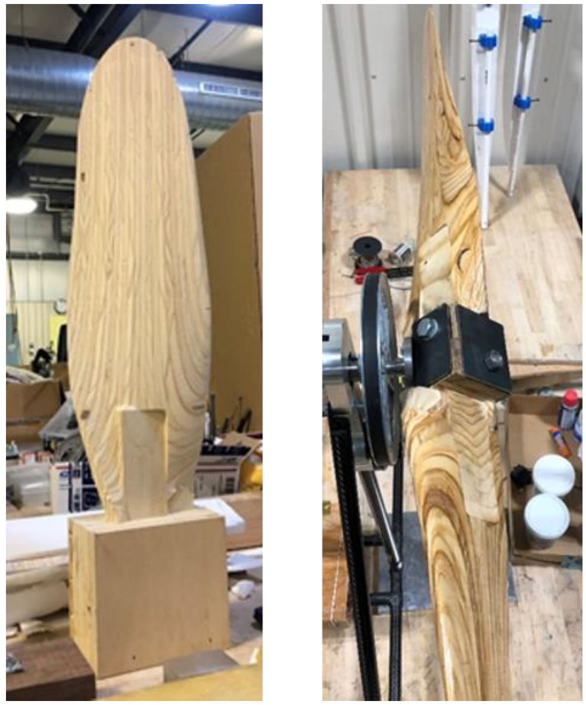

Figure 26: Fan Blade (Left) and Assembly (Right)

We then used 3 mm sheet metal brackets to keep two blades together. The final fan assembly can be seen in Figure 26.

The fan mount (see Figure 27) was also manufactured by the CNC router out of aluminum.

Figure 27: Fan Mount

FRAME FABRICATION

We initially looked into using PVC or aluminum tubes to form the frame in order to keep the cost low. Upon advice from various professors, we began to consider carbon fiber tubing, which has a very high strength to weight ratio. This would be more expensive but would allow us to bring the weight of the hull down significantly and have more strength than either PVC of aluminum would give.

When beginning manufacturing, we cut carbon fiber tubes to desired length, and then prepared their ends. This meant either sanding a curve into the end so that it could sit flush to another tube or using epoxy to fasten connectors to allow connection to the fan mount (see Figure 27). To connect the tubes to each other, we used carbon fiber wrap and epoxy to harden it in place. Difficulties with this method were that the tape tended to unravel and had to be put into the proper position very carefully. Once hardened, this created a very strong joint, as shown in Figure 28.

Figure 28: Carbon Fiber Tube Joint

ELECTRONICS POD FABRICATION

The electronics pod served to hold both our electronics (battery, remote control signal receiver) and extra weight (to bring the boat up to its target weight). It should be able to slide along the frame to affect the center of gravity. We went with a basic box design which was easily produced with plywood. The design and completed pod are shown in Figure 29.

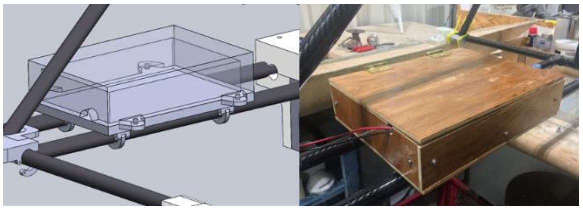

Figure 29: Electronics Pod

PROTOTYPE TESTING

Once the prototype was built, numerous tests were performed to confirm the subsystems as well as the whole prototype working as designed. Most of these tests were carried out in Cedar Lake, which is conveniently located on the campus of Cedarville University.

Firstly, the overall weight of the completed prototype was only 35 lb. The original 50 lb weight target was achieved by adding extra weights into the electronics pod.

Simply observing the waterline on the hulls when the prototype was placed in the lake water revealed the design provided enough buoyancy force to keep the device floating on the water.

The electronic system being controlled remotely worked flawlessly. When testing our remote control, we found it had a working range exceeding the longest distance across the Cedar Lake.

In order to test the drag acting on both the hulls and the hydrofoils, the hydrofoil prototype was pulled behind a boat with a fishing line. The drag force along the fishing line lifted a weight on a scale sit on the boat which was being recorded on video. This drag test setup is shown in Figure 30.

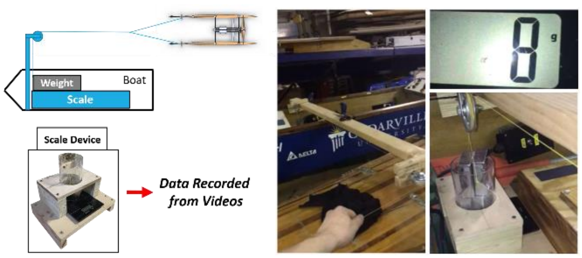

Figure 30: Drag Test Setup

The drag values were then taken by inspecting the video frames at half-second intervals. Velocity data of the boat were recorded using the data acquisition unit available on-board the boat.

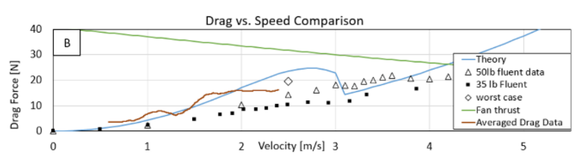

Figure 31: Comparison between Test Data (Red Curve) and Predictions (Blue Curve and Symbols)

Surprising agreement between our test data, CFD simulation results, and theory was observed as shown in Figure 31.

Unfortunately, during testing the wake induced by the boat influenced the flight of the prototype which prevented us from obtaining valid data after takeoff.

Finally we tested the complete fully-functioning hydrofoil prototype in Cedar Lake and it successfully achieved stable flight with the hulls being lifted out of the water, as shown in Figure 32.

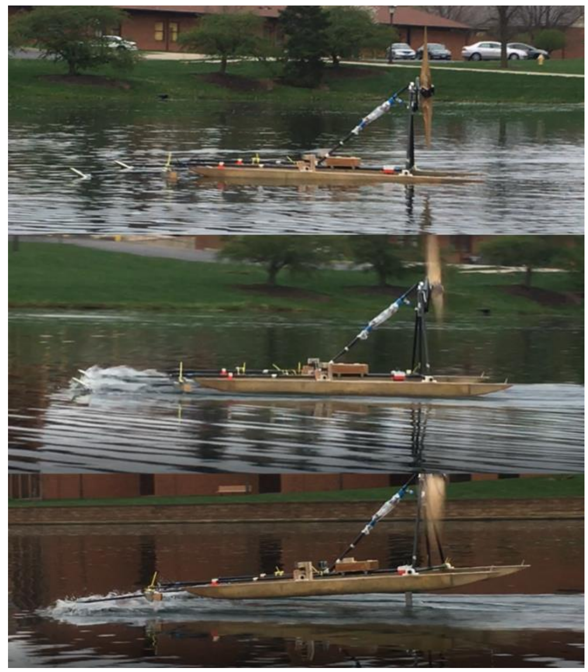

Figure 32: Steady Flight of the Hydrofoil Prototype

CONCLUSION

We achieved the initial goal of designing a half-size remote-controlled hydrofoil prototype and realized steady flight with the prototype. We are confident that we will be able to build a full-size human-powered hydrofoil boat in the coming years. Based on the experience we gained, we concluded that

- The SolidWorks Flow Simulation and the analytical drag model are accurate enough for drag prediction and hull design
- The roll stability analysis presented in the current paper seems to be valid
- A similar pitch stability analysis should be developed to better direct the surface finding mechanism design

- Fan is a simple yet effective method of propulsion. Its advantage will be more appreciable when we design the full-size boat
- A fan section profile with high lift to drag ratio is preferred in the future full-size boat design

---

Joshua Close was responsible for the hull design. He received his bachelor's degree in Mechanical Engineering from Cedarville University in 2019.

Bryan Perschbacher was responsible for the CFD simulation. He received his bachelor's degree in Mechanical Engineering from Cedarville University in 2019.

Sean Reilly was the team leader and was responsible for the hydrofoil and surface finder design. He received his bachelor's degree in Mechanical Engineering from Cedarville University in 2019.

Hunter Stevens was responsible for the frame and electronics pod design. He received his bachelor's degree in Mechanical Engineering from Cedarville University in 2019.

Jonathan Thong was responsible for the hydrofoil and strut design. He received his bachelor's degree in Mechanical Engineering at Cedarville University in 2019.

Etienne Viaud-Murat was responsible for the fan design. He received his bachelor's degree in Mechanical Engineering from Cedarville University in 2019.

Stephen Wormald was responsible for the testing. He received his bachelor's degree in Mechanical Engineering from Cedarville University in 2019.

George Qin, **Ph.D.** was the faculty advisor of the team. He received his Ph.D. in Mechanical Engineering from Iowa State University in 2007.

REFERENCES

Ikonen, M. (2011). About the Possibilities to Power Vehicles with Human Muscles. Terrassa, Spain.

Johnson, W. (2013). *Rotorcraft Aeromechanics.* Cambridge.

Katz, J., & Plotkin, A. (2001). *Low-Speed Aerodynamics.* Cambridge.

Munson. (2016). *Fundamentals of Fluid Mechanics.* Wiley.

Vellinga, R. (2009). *Hydrofoils: Design, Build, Fly* . Peacock Hill Publishing.

Wall, M. (1995). *Decavitator - Human-Powered Hydrofoil*. Retrieved from http://lancet.mit.edu/decavitator/